

This discussion paper is/has been under review for the journal *Atmospheric Chemistry and Physics (ACP)*. Please refer to the corresponding final paper in *ACP* if available.

**Mobile mini-DOAS
measurement of NO₂
& HCHO**

M. Johansson et al.

Mobile mini-DOAS measurement of the emission of NO₂ and HCHO from Mexico City

M. Johansson¹, C. Rivera¹, B. de Foy², W. Lei^{3,4}, J. Song^{3,4}, Y. Zhang¹, B. Galle¹, and L. Molina^{3,4}

¹Chalmers University of Technology, Göteborg, Sweden

²Saint Louis University, St Louis, MO, USA

³Molina Center for Energy and the Environment, La Jolla, CA, USA

⁴Massachusetts Institute of Technology, Cambridge, MA, USA

Received: 31 October 2008 – Accepted: 5 November 2008 – Published: 12 January 2009

Correspondence to: M. Johansson (mattias.johansson@chalmers.se)

Published by Copernicus Publications on behalf of the European Geosciences Union.

Title Page

Abstract

Introduction

Conclusions

References

Tables

Figures

◀

▶

◀

▶

Back

Close

Full Screen / Esc

Printer-friendly Version

Interactive Discussion



Abstract

We here present the result of one mobile measurement using two ground based zenith viewing Differential Optical Absorption Spectroscopy (DOAS) instrument performed in a cross-section of the plume from the MCMA on the 10 March 2006 as part of the MILAGRO field campaign. The two instruments operated in the UV and the visible wavelength region respectively and have been used to derive the differential vertical columns of HCHO and NO₂ above the measurement route.

Using a mass-averaged wind speed and wind direction from the WRF model the instantaneous flux of HCHO and NO₂ has been calculated from the two measurements and the results compared to the CAMx chemical model. The calculated flux through the measured cross-section was 1.9 (1.5–2.2) kg/s of HCHO and 4.4 (4.0–5.0) kg/s of NO₂ using the UV instrument and 3.66 (3.63–3.73) kg/s of NO₂ using the visible light instrument. The comparison with modeled values from CAMx shows a good agreement for the outflow of both NO₂ and HCHO at this occasion.

1 Introduction

Formaldehyde (HCHO) is the most abundant carbonyl in ambient air and can reach concentrations of up to 60 ppb in polluted air (Finlayson-Pitts and Pitts, 1999). Being both carcinogenic (Vaughan et al., 1986a,b; Hauptmann et al., 2003) and soluble in water, it is easily absorbed by the human respiratory system and has a major impact on residents in polluted areas. HCHO is emitted both directly (primary HCHO) as a result of incomplete combustion and generated in the atmosphere (secondary HCHO) in the oxidation of the most common VOCs (Finlayson-Pitts and Pitts, 1999; Garcia et al., 2006). Mainly due to photolysis by UV-light below 360 nm and reaction with OH, HCHO has a lifetime in ambient air of a few hours. Its oxidation chain leads to the formation of OH and HO₂, for which it can be one of the major producers in polluted air (Atkinson 2000; Volkamer et al., 2005).

ACPD

9, 865–882, 2009

Mobile mini-DOAS measurement of NO₂ & HCHO

M. Johansson et al.

Title Page

Abstract

Introduction

Conclusions

References

Tables

Figures

◀

▶

◀

▶

Back

Close

Full Screen / Esc

Printer-friendly Version

Interactive Discussion



**Mobile mini-DOAS
measurement of NO₂
& HCHO**

M. Johansson et al.

Title Page

Abstract

Introduction

Conclusions

References

Tables

Figures

◀

▶

◀

▶

Back

Close

Full Screen / Esc

Printer-friendly Version

Interactive Discussion

Mexico City is located at 19.4 latitude and elevation of 2200 m approximately, within a basin on the central Mexican plateau (Fast et al., 2007). Mexico City presents severe air pollution problems and is one of the most polluted cities in the world. Formaldehyde levels in Mexico City, both indoor and outdoor have been extensively studied, revealing higher mean concentrations in indoor air (Baez et al., 2003, 2006) and formaldehyde as the most abundant aldehyde both in indoor and outdoor air (Baez et al., 2006). Studies reveal a decrease in formaldehyde levels in Mexico City since the beginning of the 1990s (Baez et al., 2003, 2006, 1995), however they are still among the highest reported in the literature (Baez et al., 1995). Typical observed formaldehyde concentrations downtown Mexico City are between 12.7–23.9 ppb (Madronich, 2006; Grutter et al., 2005); however mean values above 40 ppb and peak values of 110 ppb have been also reported, finding the maximum concentrations between 10:00–12:00 h, indicating primary emissions probably from motor vehicles during rush hours (Baez et al., 1995). Studies of in-vehicle formaldehyde exposure in Mexico City using different transportation modes indicate higher level of exposure in microbus than in car, bus and metro (Shiohara et al., 2005).

The MILAGRO (Megacity Initiative, Local and Global Research Observations) field campaign held in the Mexico City Metropolitan Area (MCMA) during March 2006 was aimed at characterizing the chemical processes leading to the formation of photochemical smog in the MCMA.

The 10 March 2006 was characterized by mostly sunny and dry conditions, no deep convection, clear mountains in the vicinity of Mexico City and periods of cirrus clouds (Fast et al., 2007). In addition, the 10 March was a period with the most direct transport towards the northeast (Fast et al., 2007; Doran et al., 2007).

The Differential Optical Absorption Spectroscopy (DOAS) technique has for a long time been used to measure HCHO levels in ambient air, both using active instruments (Platt et al., 1979; Hak et al., 2005) and passive instruments (Heckel et al., 2005).

2 Experimental

The mobile mini-DOAS instrument (described by Galle et al., 2002) uses a telescope to collect zenith scattered light in the UV or visible region. This light is through an optical quartz fibre led into a miniaturized spectrometer (Fig. 1). The spectrometer is connected to a laptop which stores the spectra and simultaneously stores the position using an attached GPS-receiver.

Each measured spectrum is ratioed to a Fraunhofer reference spectrum and the DOAS evaluation yields the difference in total vertical column, the integral over the concentration along a vertical line from the instrument and up, between the measured spectrum and the chosen Fraunhofer reference spectrum. If the measurement has passed underneath a gas plume then the flux of the plume can be calculated by integrating the total number of molecules in the cross section of the plume, multiplying with the wind speed and correcting for the angle between the wind direction and the traverse direction.

During the MILAGRO field campaign, a car equipped with two mobile mini-DOAS instruments, one measuring in the UV (280 to 425 nm) and one in the visible (340 to 480 nm), performed measurements in the MCMA to capture the distribution and possible outflow of air pollutants. On the 10 March 2006, a measurement was made on the entire width of the plume flowing out of the Mexico City basin.

The spectra collected with the UV-spectrometer has been evaluated for NO₂ (using the NO₂ cross section by Vandaele et al., 1998) and HCHO (using the HCHO cross section by Meller and Moortgat, 2000) in the wavelength range 311 to 347 nm using the DOAS technique and the WinDOAS software package (Van Roozendaal and Fayt, 2001). To increase signal to noise ratio, the collected spectra have been co-added giving 900 single exposures in each evaluated spectrum and a time-resolution of the measurement of slightly less than two minutes. Included into the fit were also the cross sections of SO₂ (Bogumil et al., 2003), O₃ (223 K) (Burrows et al., 1999), O₃ (293 K) (Burrows et al., 1999), O₄ (Hermans et al., 1999) and a synthetic Ring spectrum gen-

Mobile mini-DOAS measurement of NO₂ & HCHO

M. Johansson et al.

Title Page

Abstract

Introduction

Conclusions

References

Tables

Figures

◀

▶

◀

▶

Back

Close

Full Screen / Esc

Printer-friendly Version

Interactive Discussion



erated from the measured Fraunhofer reference spectrum using the DOASIS software (DOASIS – Kraus). An example of a DOAS-fit in the wavelength range 311 to 347 nm can be seen in Fig. 2.

The spectra collected with the visible light spectrometer has been evaluated for NO₂ in the wavelength range 410 to 460 nm using the DOAS technique and the WinDOAS software (Van Roozendael and Fayt, 2001). Also these spectra have been co-added to increase the signal to noise ratio, giving 2240 single exposures in each evaluated spectrum and a time-resolution of slightly less than two minutes. Included into the fit were also the cross section of O₄ (Hermans et al., 1999) and a synthetic Ring spectrum calculated using the DOASIS software (DOASIS – Kraus).

Estimation of the pollutant fluxes requires knowledge of the horizontal wind flux. For this purpose, the WRF mesoscale meteorological model was used to simulate the local meteorological conditions in the Mexico City basin. Three grids were used with resolutions of 36 km covering the whole of Mexico, 12 km covering the region around the MCMA (including the Gulf and the Pacific Ocean) and 3 km covering the MCMA basin and immediate surroundings. In the vertical, 51 levels were used with the model top at ~7 km a.g.l. The land surface provides an important forcing term for the local winds in the basin. In order to capture these, high resolution data from MODIS was used to initialize the land use, vegetation fraction, surface albedo and soil temperature (de Foy et al., 2006). The WRF model contains certain hard-coded modifications to handle urban surfaces. These however were not found to be representative of Mexico City and were removed. The NOAA land surface model was used together with the YSU boundary layer scheme and Kain-Fritsch convection. The z-diffusion scheme was used for the fine grid only.

Horizontal wind flux was calculated based on mass-averaged fluxes in the meridional and zonal directions. This was performed for the column below the simulated boundary layer height at the grid column closest to the measured column. This horizontal wind flux was then used to estimate the flux of NO₂ and HCHO through the measured cross-section.

**Mobile mini-DOAS
measurement of NO₂
& HCHO**M. Johansson et al.

Title Page

Abstract

Introduction

Conclusions

References

Tables

Figures

⏪

⏩

◀

▶

Back

Close

Full Screen / Esc

Printer-friendly Version

Interactive Discussion



**Mobile mini-DOAS
measurement of NO₂
& HCHO**

M. Johansson et al.

[Title Page](#)[Abstract](#)[Introduction](#)[Conclusions](#)[References](#)[Tables](#)[Figures](#)[◀](#)[▶](#)[◀](#)[▶](#)[Back](#)[Close](#)[Full Screen / Esc](#)[Printer-friendly Version](#)[Interactive Discussion](#)

The measured columns have been compared to the simulation results for the Comprehensive Air Quality Model with Extensions (CAMx, [Environ International Corporation, 2008]) chemical model which was setup for the region surrounding the MCMA during the MILAGRO campaign. CAMx was driven by hourly prognostic meteorological fields from WRF. The CAMx domain configuration was similar to the WRF D3 except for a smaller domain of 70×70 grids, and emission estimates were constructed from the official emission inventory for the year 2006 for MCMA, and were adjusted based on the NO_x and CO measurements from a local monitoring network and the extensive VOC measurements during the MILAGRO-2006 campaign. The simulated columns of NO₂ and HCHO have been bi-linearly interpolated in space and linearly interpolated in time along the mobile track from the 1-h average concentration fields of the model output to be able to compare the distribution of NO₂ or HCHO along the measurement route.

3 Results and discussion

The evaluated measurement was performed on the 10 March 2006 starting at 12:58 local time (18:58 UTC).

Figure 3 shows the evaluated differential columns of NO₂ from both the UV and the visible light spectrometer together with the extracted columns of NO₂ from the CAMx model. The derived differential NO₂ columns from the UV spectrometer are somewhat higher than from the visible light spectrometer. This is most likely due to somewhat longer path lengths in the UV than in the visible due to the higher cross section for Rayleigh and Mie scattering. However the difference between the two measurements is less than 2σ of the spectral fit from the UV measurement.

By using the mass-averaged wind-speed and wind-direction from the WRF-model, the flux of NO₂ through the measured cross-section of the plume can be estimated from both of the two DOAS-instruments, see Table 1. The same estimation can be done for the modeled columns, however for the results to be comparable must the modeled

columns be transformed into differential columns. This has been by subtracting the lowest modeled column value from all other modeled values, the resulting flux can be seen in Table 1. The CAMx model shows a flux very well in agreement with the measurements, however with a difference in the distribution of NO₂ along the measurement route. The model shows a broader and lower plume than does the measurements and with a peak located approximately 10 km from the location of the measured peak.

Figure 4 shows the evaluated differential columns of HCHO from the UV spectrometer and the extracted columns of HCHO from the CAMx model, the route of the measurement is seen in Fig. 5. By using the mass-averaged wind-speed and wind-direction from the WRF-model, the flux of HCHO through the measured cross-section of the city-plume can be calculated from the DOAS-measurement and the differentiated columns from the CAMx model see Table 2. The error range for the flux calculated from the DOAS-instrument has been calculated by error propagation of the error from the spectral fit.

The CAMx model shows a high background concentration of HCHO together with a small increase in columns in the city plume. To be comparable with the measurement, the modeled columns are transformed into differential columns by subtracting the first column from all other. Doing so results in a very much smaller modeled plume, with a flux of 0.5 kg/s, almost 75% lower than the measured. However, if instead the HCHO column upwind Mexico City, around 8×10^{15} molecules/cm², is subtracted from each modeled column a flux of 1.1 kg/s is obtained. The large difference between the two results is probably due to the wider plume obtained from the model.

The large difference in the peak and spatial and temporal distribution of the HCHO and NO₂ columns in the model is probably due to the source differences in HCHO and NO₂ and the impacts of meteorology and terrain. The NO₂ column originated from the emissions and goes through the NO_y inter-conversion, but HCHO is attributed to both emissions and photochemical production. Under certain circumstances, the dispersion and transport can smooth and spread out the secondary HCHO plume when the plume moves over a complex terrain.

**Mobile mini-DOAS
measurement of NO₂
& HCHO**M. Johansson et al.

[Title Page](#)[Abstract](#)[Introduction](#)[Conclusions](#)[References](#)[Tables](#)[Figures](#)[⏪](#)[⏩](#)[◀](#)[▶](#)[Back](#)[Close](#)[Full Screen / Esc](#)[Printer-friendly Version](#)[Interactive Discussion](#)

The collected spectra have also been evaluated for O₄ both in the UV and the visible wavelength range and neither of the ranges shows differential O₄ columns above the detection limit and thus no obvious elongation of the optical path length due to radiative transport (Johansson et al., 2008; Wagner et al., 2004).

4 Conclusions

We have in this paper presented results from a mobile mini-DOAS measurement made on the 10 March 2006, during the MILAGRO field campaign. The measurement resulted in an estimation of the instantaneous outflow of NO₂ and HCHO from the entire MCMA. These fluxes have been compared to modeled columns using the CAMx model. The comparison shows a good agreement for the outflow of NO₂ and HCHO.

Acknowledgements. We thank M. Zavala and N. Bei at the Molina Center for Energy and the Environment for assisting in producing the emission data and meteorological data used for CAMx runs. We thank the Swedish International Development Cooperation Agency (SIDA) and the US National Science Foundation (ATM-0528227 and ATM-0411803) for funding of this research.

References

- Atkinson, R.: Atmospheric chemistry of VOCs and NO_x, *Atmos. Environ.*, 34, 2063–2101, 2000.
- Baez, A., Padilla, H., Garcia, R., Torres, M., Rosas, I., and Belmont, R.: Carbonyl levels in indoor and outdoor air in Mexico City and Xalapa, Mexico, *Sci. Total Environ.*, 302, 211–226, 2003.
- Baez, A. P., Belmont, R., and Padilla, H.: Measurements of formaldehyde and acetaldehyde in the atmosphere of Mexico City, *Environ. Pollut.*, 89, 163–167, 1995.
- Baez, A. P., Padilla, H., Garcia, R., Belmont, R., and Torres, M.: Measurement of indoor-outdoor carbonyls at four residential homes in Mexico City Metropolitan Area, *Int. J. Environ. Pollut.*, 26, 90–105, 2006.

Mobile mini-DOAS measurement of NO₂ & HCHO

M. Johansson et al.

Title Page

Abstract

Introduction

Conclusions

References

Tables

Figures

◀

▶

◀

▶

Back

Close

Full Screen / Esc

Printer-friendly Version

Interactive Discussion



**Mobile mini-DOAS
measurement of NO₂
& HCHO**

M. Johansson et al.

Title Page

Abstract

Introduction

Conclusions

References

Tables

Figures

◀

▶

◀

▶

Back

Close

Full Screen / Esc

Printer-friendly Version

Interactive Discussion



Bogumil, K., Orphal, J., Homann, T., Voigt, S., Spietz, P., Fleischmann, O. P., Vogel, A., Hartmann, M., Bovensmann, H., Frerik, J., and Burrows, J. P.: Measurements of Molecular Absorption Spectra with the SCIAMACHY PreFlight Model: Instrument Characterization and Reference Data for Atmospheric Remote-Sensing in the 230–2380 nm Region, *J. Photoch. Photobio. A*, 157, 167–184, 2003.

Burrows, J. P., Richter, A., Dehn, A., Deters, B., Himmelmann, S., Voigt, S., and Orphal, J.: Atmospheric remote sensing reference data from GOME: 2. Temperature dependent absorption cross sections of O₃ in the 231–794 nm range, *J. Quant. Spectrosc. Ra.*, 61, 509–517, 1999.

de Foy, B., Molina, L. T., and Molina, M. J.: Satellite-derived land surface parameters for mesoscale modelling of the Mexico City basin, *Atmos. Chem. Phys.*, 6, 1315–1330, 2006, <http://www.atmos-chem-phys.net/6/1315/2006/>.

Doran, J. C., Barnard, J. C., Arnott, W. P., Cary, R., Coulter, R., Fast, J. D., Kassianov, E. I., Kleinman, L., Laulainen, N. S., Martin, T., Paredes-Miranda, G., Pekour, M. S., Shaw, W. J., Smith, D. F., Springston, S. R., and Yu, X.-Y.: The T1-T2 study: evolution of aerosol properties downwind of Mexico City, *Atmos. Chem. Phys.*, 7, 1585–1598, 2007, <http://www.atmos-chem-phys.net/7/1585/2007/>.

Comprehensive Air Quality Model with Extensions (CAMx): ver 4.5. Programmed by Environ International Corporation, available at <http://www.camx.com>, 2008.

Fast, J. D., de Foy, B., Acevedo Rosas, F., Caetano, E., Carmichael, G., Emmons, L., McKenna, D., Mena, M., Skamarock, W., Tie, X., Coulter, R. L., Barnard, J. C., Wiedinmyer, C., and Madronich, S.: A meteorological overview of the MILAGRO field campaigns, *Atmos. Chem. Phys.*, 7, 2233–2257, 2007, <http://www.atmos-chem-phys.net/7/2233/2007/>.

Finlayson-Pitts, B. J. and Pitts, J. N.: *Chemistry of the Upper and Lower Atmosphere: Theory, Experiments, and Applications*, Academic Press, San Diego, USA, 1999.

Galle, B., Oppenheimer, C., Geyer, A., McGonigle, A. J. S., Edmonds, M., and Horrocks, L.: A miniaturised ultraviolet spectrometer for remote sensing of SO₂ fluxes: A new tool for volcano surveillance, *J. Volcanol. Geoth. Res.*, 119, 241–254, 2002.

Garcia, A. R., Volkamer, R., Molina, L. T., Molina, M. J., Samuelson, J., Mellqvist, J., Galle, B., Herndon, S. C., and Kolb, C. E.: Separation of emitted and photochemical formaldehyde in Mexico City using a statistical analysis and a new pair of gas-phase tracers, *Atmos. Chem. Phys.*, 6, 4545–4557, 2006,

<http://www.atmos-chem-phys.net/6/4545/2006/>.

Grutter, M., Flores, E., Andraca-Ayala, G., and Baez, A.: Formaldehyde levels in downtown Mexico City during 2003., *Atmos. Environ.*, 39, 1027–1034, 2005.

5 Hak, C., Pundt, I., Trick, S., Kern, C., Platt, U., Dommen, J., Ordóñez, C., Prévôt, A. S. H., Junkermann, W., Astorga-Lloréns, C., Larsen, B. R., Mellqvist, J., Strandberg, A., Yu, Y., Galle, B., Kleffmann, J., Lörzer, J. C., Braathen, G. O., and Volkamer, R.: Intercomparison of four different in-situ techniques for ambient formaldehyde measurements in urban air, *Atmos. Chem. Phys.*, 5, 2881–2900, 2005,
<http://www.atmos-chem-phys.net/5/2881/2005/>.

10 Hauptmann, M., Lubin, J. H., Stewart, P. A., Hayes, R. B., and Blair, A.: Mortality from lymphohematopoietic malignancies among workers in formaldehyde industries, *J. Natl. Cancer I.*, 95, 1615–1623, 2003.

Wittrock, F., Oetjen, H., Richter, A., Fietkau, S., Medeke, T., Rozanov, A., and Burrows, J. P.: MAX-DOAS measurements of atmospheric trace gases in Ny-Ålesund – Radiative transfer studies and their application, *Atmos. Chem. Phys.*, 4, 955–966, 2004,
<http://www.atmos-chem-phys.net/4/955/2004/>.

15 Hermans, C., Vandaele, A. C., Carleer, M., Fally, S., Colin, R., Jenouvrier, A., Coquart, B., and Mérienne, M.-F.: Absorption cross-sections of atmospheric constituents: NO₂, O₂, and H₂O, *Environ. Sci. Pollut. R.*, 6, 151–158, 1999.

20 Johansson, M., Galle, B., Yu, T., Tang, L., Chen, D., Li, H., Li, J. X., and Zhang, Y.: Quantification of total emission of air pollutants from Beijing using mobile mini-DOAS, *Atmos. Environ.*, 42, 6926–6933, 2008.

DOASIS ver 3.2.2734: Programmed by Kraus, S., available at: <http://www.iup.uni-heidelberg.de/bugtracker/projects/doasis/>, 2007.

25 Madronich, S.: Chemical evolution of gaseous air pollutants down-wind of tropical megacities: Mexico City case study, *Atmos. Environ.*, 40, 6012–6018, 2006.

Meller, R. and Moortgat, G. K.: Temperature dependence of the absorption cross sections of formaldehyde between 223 and 323 K in the wavelength range 225–375 nm, *J. Geophys. Res.*, 105, 7089–7101, 2000.

30 Platt, U., Perner, D., and Pätz, H. W.: Simultaneous measurement of atmospheric CH₂O, O₃ and NO₂ by differential optical absorption, *J. Geophys. Res.*, 84, 6329–6335, 1979.

Shiohara, N., Fernandez-Bremauntz, A. A., Blanco-Jimenez, S., and Yanagisawa, Y.: The commuters' exposure to volatile chemicals and carcinogenic risk in Mexico City, *Atmos. Environ.*,

ACPD

9, 865–882, 2009

Mobile mini-DOAS measurement of NO₂ & HCHO

M. Johansson et al.

Title Page

Abstract

Introduction

Conclusions

References

Tables

Figures

◀

▶

◀

▶

Back

Close

Full Screen / Esc

Printer-friendly Version

Interactive Discussion



39, 3481–3489, 2005.

Wagner, T., Dix, B., Friedeburg, C. V., Frieß, U., Sanghavi, S., Sinreich, R., and Platt, U.: MAX-DOAS O₄ measurements: A new technique to derive information on atmospheric aerosols – principles and information content, *J. Geophys. Res.-Atmos.*, 109, 1–19, 2004.

5 Van Roozendaal, M. and Fayt, C.: WinDOAS 2.1 Software User Manual, BIRA-IASB, 2001.

Vandaele, A. C., Hermans, C., Simon, P. C., Carleer, M., Colin, R., Fally, S., Merienne, M. F., Jenouvrier, A., and Coquart, B.: Measurements of the NO₂ absorption cross-section from 42 000 cm⁻¹ to 10 000 cm⁻¹ (238–1000 nm) at 220 K and 294 K, *J. Quant. Spectrosc. Ra., Atmos. Spec. Appl.*, 96, 59, 171–184, 1998.

10 Vaughan, T. L., Strader, C., Davis, S., and Daling, J. R.: Formaldehyde and cancers of the pharynx, sinus and nasal cavity. 1. Occupational exposures, *Int. J. Cancer*, 38, 677–683, 1986a.

Vaughan, T. L., Strader, C., Davis, S., and Daling, J. R.: Formaldehyde and cancers of the pharynx, sinus and nasal cavity. 2. Residential exposures, *Int. J. Cancer*, 38, 685–688, 1986b.

15 Volkamer, R., Molina, L. T., Molina, M. J., Shirley, T., and Brune, W. H.: DOAS measurement of glyoxal as an indicator for fast VOC chemistry in urban air, *Geophys. Res. Lett.*, 32, L08806, doi:10.1029/2005GL022616, 2005.

ACPD

9, 865–882, 2009

Mobile mini-DOAS measurement of NO₂ & HCHO

M. Johansson et al.

Title Page

Abstract

Introduction

Conclusions

References

Tables

Figures

◀

▶

◀

▶

Back

Close

Full Screen / Esc

Printer-friendly Version

Interactive Discussion



**Mobile mini-DOAS
measurement of NO₂
& HCHO**

M. Johansson et al.

Table 1. Estimated NO₂ fluxes from the two instruments and CAMx using the mass-averaged wind-speed and wind-direction from the WRF model.

Instrument	Flux [kg/s]
UV-spectrometer	4.4 (4.0–5.0)
Vis-spectrometer	3.66 (3.63–3.73)
CAMx	3.6

[Title Page](#)[Abstract](#)[Introduction](#)[Conclusions](#)[References](#)[Tables](#)[Figures](#)[I ◀](#)[▶ I](#)[◀](#)[▶](#)[Back](#)[Close](#)[Full Screen / Esc](#)[Printer-friendly Version](#)[Interactive Discussion](#)

**Mobile mini-DOAS
measurement of NO₂
& HCHO**

M. Johansson et al.

Table 2. Estimated HCHO fluxes from the DOAS instrument and the CAMx chemical model using the mass-averaged wind-speed and wind-direction from the WRF model.

Instrument	Flux [kg/s]
UV-spectrometer	1.9 (1.5–2.2)
CAMx	1.1

[Title Page](#)[Abstract](#)[Introduction](#)[Conclusions](#)[References](#)[Tables](#)[Figures](#)[I ◀](#)[▶ I](#)[◀](#)[▶](#)[Back](#)[Close](#)[Full Screen / Esc](#)[Printer-friendly Version](#)[Interactive Discussion](#)

**Mobile mini-DOAS
measurement of NO₂
& HCHO**

M. Johansson et al.

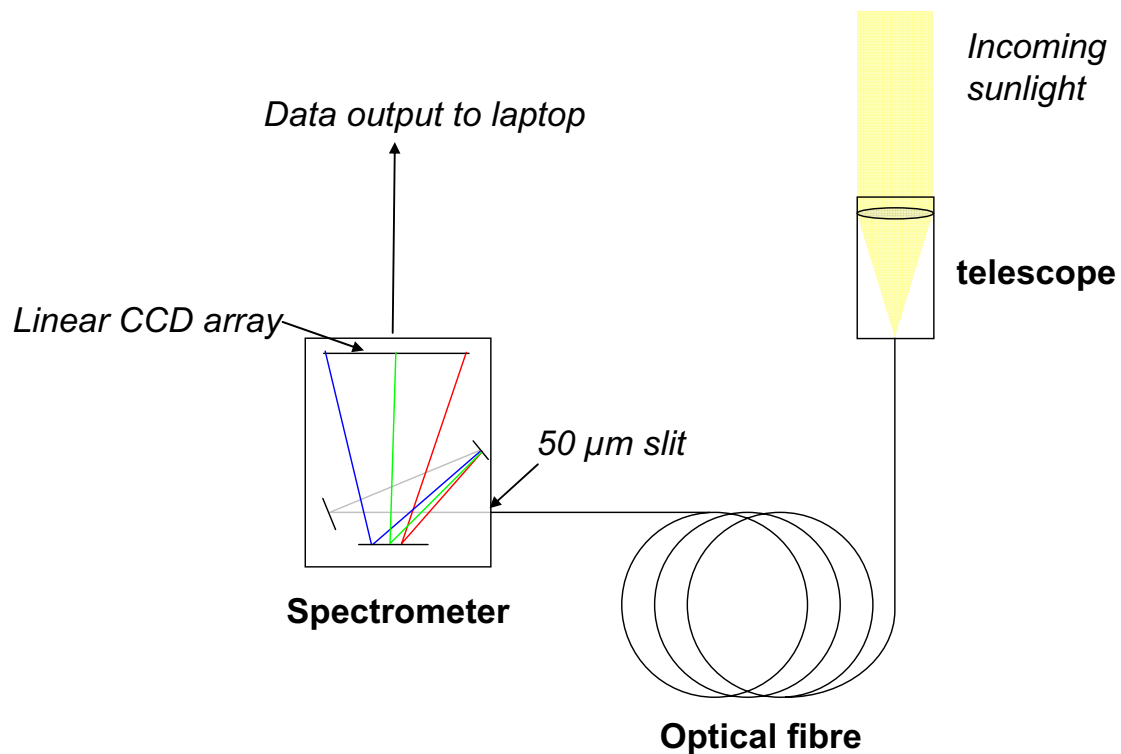


Fig. 1. The mobile Mini-DOAS instrument collects zenith scattered light.

[Title Page](#)[Abstract](#)[Introduction](#)[Conclusions](#)[References](#)[Tables](#)[Figures](#)[◀](#)[▶](#)[◀](#)[▶](#)[Back](#)[Close](#)[Full Screen / Esc](#)[Printer-friendly Version](#)[Interactive Discussion](#)

**Mobile mini-DOAS
measurement of NO₂
& HCHO**

M. Johansson et al.

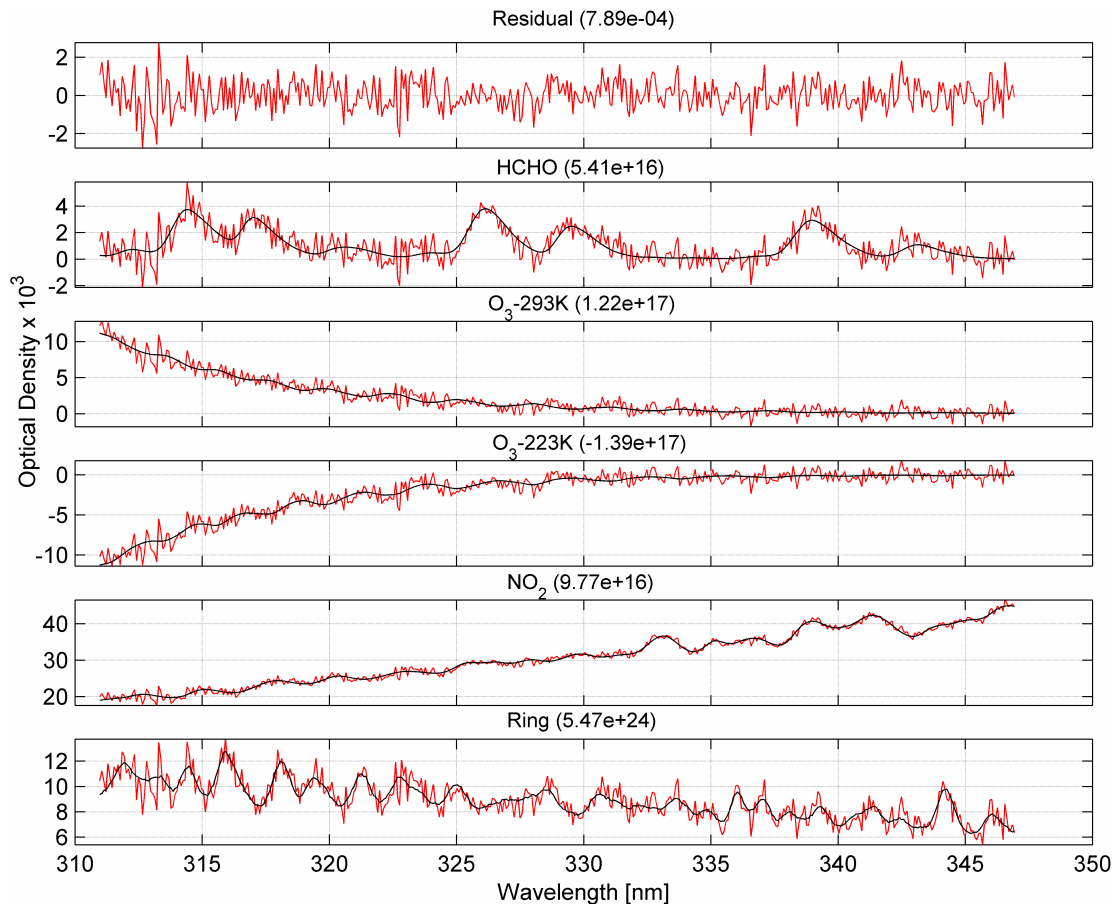


Fig. 2. The result of the DOAS fit in the 311 to 347 nm region. Top graph shows the residual of the fit, below are the fitted cross sections (from top to bottom); HCHO, O₃ (293 K), O₃ (223 K), NO₂ and a synthetic ring spectrum.

[Title Page](#)[Abstract](#)[Introduction](#)[Conclusions](#)[References](#)[Tables](#)[Figures](#)[◀](#)[▶](#)[◀](#)[▶](#)[Back](#)[Close](#)[Full Screen / Esc](#)[Printer-friendly Version](#)[Interactive Discussion](#)

**Mobile mini-DOAS
measurement of NO₂
& HCHO**

M. Johansson et al.

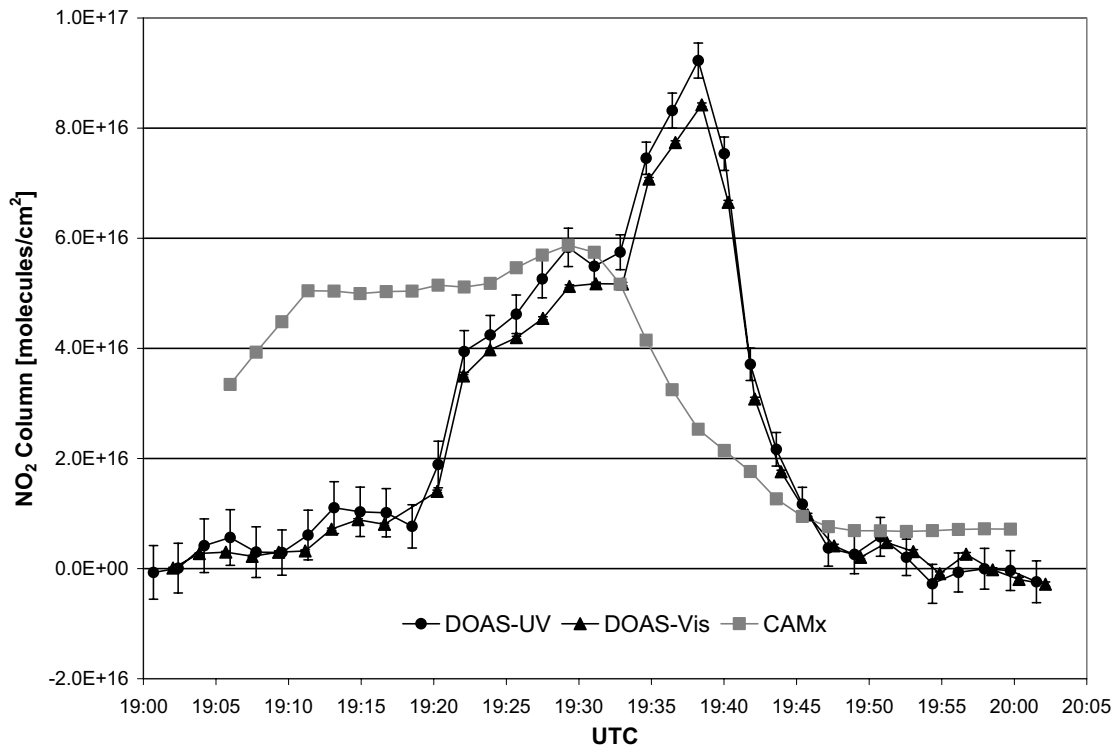


Fig. 3. Derived differential columns of NO₂ from the DOAS instrument working in the UV-region (black circles), the DOAS instrument working in the visible region (black triangles) and extracted columns of NO₂ from the CAMx model (grey squares). Notice that the modeled columns are not differential.

[Title Page](#)[Abstract](#)[Introduction](#)[Conclusions](#)[References](#)[Tables](#)[Figures](#)[◀](#)[▶](#)[◀](#)[▶](#)[Back](#)[Close](#)[Full Screen / Esc](#)[Printer-friendly Version](#)[Interactive Discussion](#)

**Mobile mini-DOAS
measurement of NO₂
& HCHO**

M. Johansson et al.

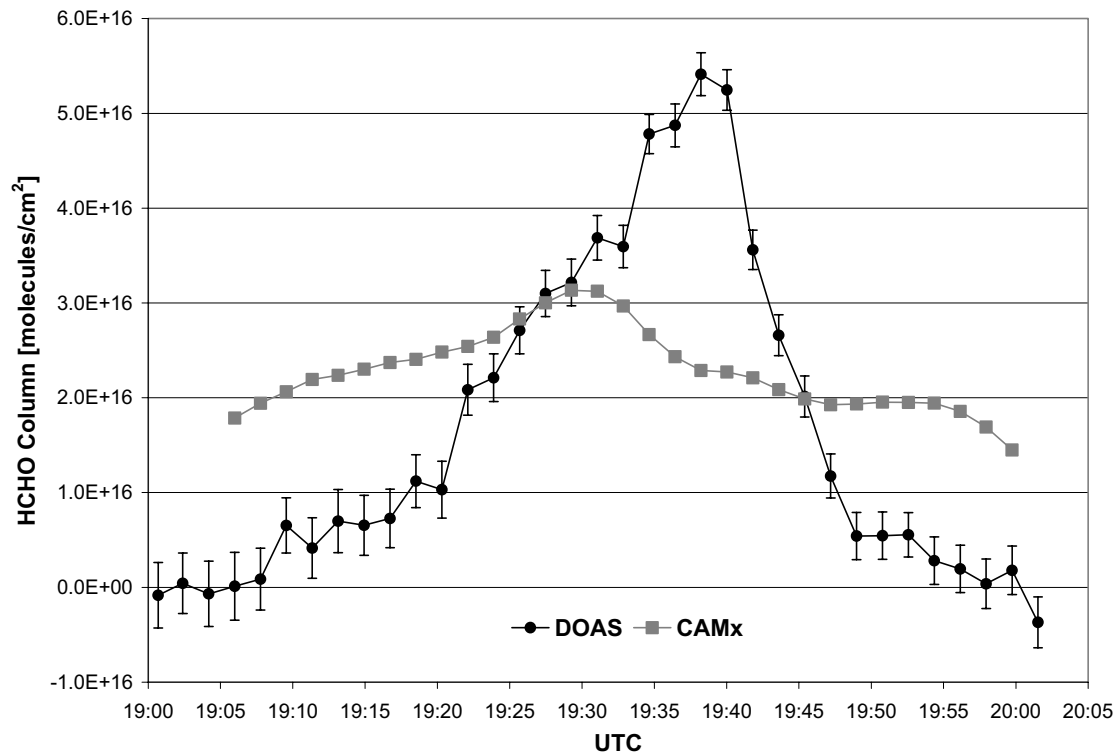


Fig. 4. Evaluated differential column of HCHO from the DOAS instrument working in the UV-region (black circles) and extracted columns of HCHO from CAMx (gray squares). Notice that the modeled columns are not differential.

[Title Page](#)[Abstract](#)[Introduction](#)[Conclusions](#)[References](#)[Tables](#)[Figures](#)[◀](#)[▶](#)[◀](#)[▶](#)[Back](#)[Close](#)[Full Screen / Esc](#)[Printer-friendly Version](#)[Interactive Discussion](#)

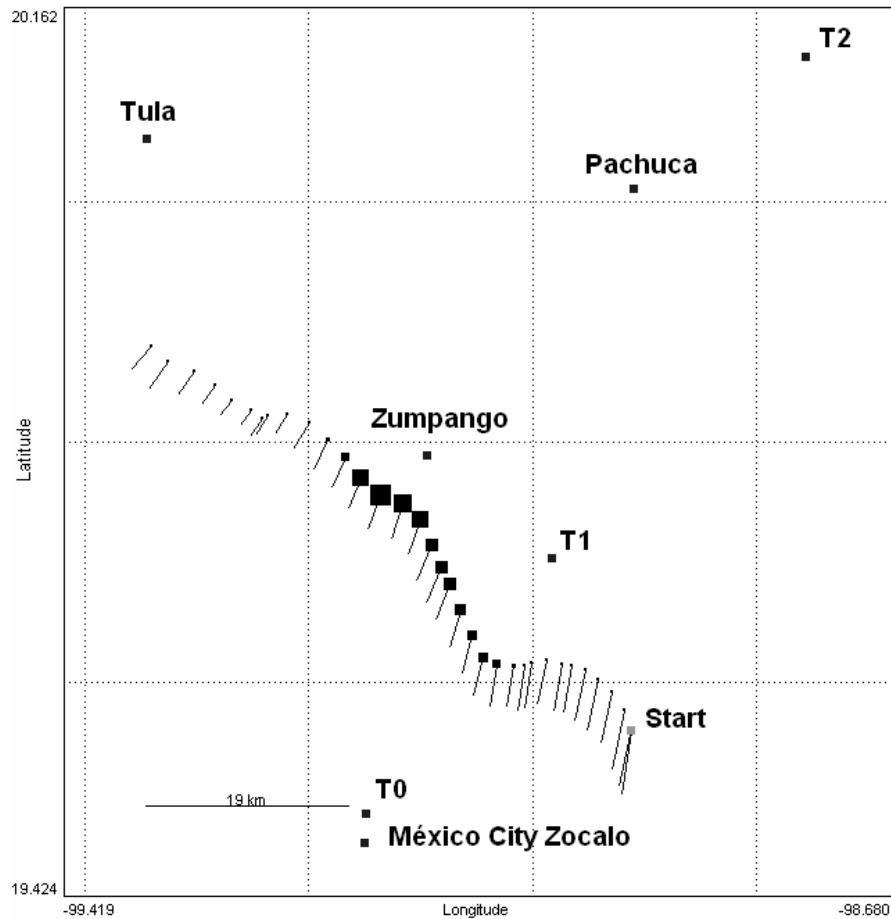


Fig. 5. The route for the HCHO measurement shown in Fig. 4. Larger differential HCHO columns are shown as larger squares, smaller columns as smaller squares. The direction from which the wind comes is marked as lines starting at each measurement point.

Mobile mini-DOAS
measurement of NO₂
& HCHO

M. Johansson et al.

Title Page

Abstract

Introduction

Conclusions

References

Tables

Figures

◀

▶

◀

▶

Back

Close

Full Screen / Esc

Printer-friendly Version

Interactive Discussion

